Available online at www.sciencedirect.com
ScienceDirect
Journal of the European Ceramic Society 30 (2010) 3311–3318
www.elsevier.com/locate/jeurceramsoc

Single and polycrystalline mullite fibres grown by laser floating zone technique

R.G. Carvalho [a], A.J.S. Fernandes [a], F.J. Oliveira [b], E. Alves [c], N. Franco [c], C. Louro [d], R.F. Silva [b], F.M. Costa [a,*]

[a] *I3N, Physics Department, University of Aveiro, 3810-193 Aveiro, Portugal*
[b] *CICECO, Glass and Ceramic Engineering Department, University of Aveiro, 3810-193 Aveiro, Portugal*
[c] *ITN, Technologic and Nuclear Institute, 2686-953 Sacavém, Portugal*
[d] *CEMUC, Mechanical Engineering Department, University of Coimbra, 3030-788 Coimbra, Portugal*

Received 10 May 2010; received in revised form 12 July 2010; accepted 22 July 2010
Available online 22 August 2010

Abstract

The laser floating zone technique was used to grow large $2Al_2O_3$–SiO_2 mullite fibres (up to 1.6 mm in diameter and 40 mm in length). The fibres grown at 10 mm/h are single crystalline in nature, while those pulled at higher rates (40 and 100 mm/h) are polycrystalline with a cellular microstructure. The crystals are highly [0 0 1] textured with respect to the fibre axis, as determined by X-ray diffraction analysis. The Raman spectra taken at different orientations corroborate the strong anisotropy observed by X-ray and SEM on both single crystalline and textured polycrystalline samples.

Four point bending tests and ultramicroindentation Vickers experiments were performed at room temperature in order to characterize the mechanical properties. The presence of lamellar inclusions in the single crystalline fibres decreases the flexural strength (431 MPa) and the fracture toughness (1.2 MPa.m$^{1/2}$) compared to the polycrystalline ones (631 MPa and 1.6 MPa.m$^{1/2}$). However, the absence of grain boundaries in the single crystals leads to higher ultramicrohardness (H_V = 15.6 GPa) and Young's modulus (E = 170 GPa) than those of the polycrystalline fibres (14.2 and 145 GPa), where a glassy intergranular phase exists.
© 2010 Elsevier Ltd. All rights reserved.

Keywords: Laser floating zone; Mullite; Fibres; Mechanical properties; Structural applications

1. Introduction

Mullite possesses many attractive properties like high melting temperature, low thermal conductivity, low thermal expansion, low dielectric constant, good thermal shock resistance, and excellent chemical inertness along with high mechanical strength at high temperatures. Extensive information on these features can be found in "Mullite", a book edited by Schneider and Komarneni,[1] and in the recent review by Schneider et al.[2]

One of the main applications of mullite is as reinforcement phase in creep resistant composite materials, namely for aerospace applications. Despite polycrystalline mullite fibres have been usually employed for reinforcement, single crystal or textured fibres exhibit better properties than amorphous or polycrystalline ones.[1,3] The benefit of single crystal fibres results from the absence of grain boundaries, avoiding high temperature mechanical deformation caused by cation and oxygen diffusion along grain boundaries.[3,4]

Mullite single crystals (MSCs) have been produced using different techniques: (i) Czochralski method; (ii) internal crystallization method (ICM) and (iii) laser floating zone (LFZ) or laser heated pedestal growth (LHPG) techniques.

The Czochralski method was used in the first successful attempt to grow MSCs by Guse and Mateika,[5] who obtained 2:1 ($2Al_2O_3 \cdot SiO_2$) crystals at 1.5 mm/h. The largest crystals achieved, up to 2 cm in diameter and 6 cm long, were inclusion-free, presenting [1 0 0] or [0 0 1] growth direction along the fibre axis. The process was carried out in nitrogen environment under

* Corresponding author.
E-mail address: flor@ua.pt (F.M. Costa).

0955-2219/$ – see front matter © 2010 Elsevier Ltd. All rights reserved.
doi:10.1016/j.jeurceramsoc.2010.07.033

normal atmospheric pressure. The same technique was used to grow the MSCs characterized in several works published by the group led by Prof. Schneider.[1,2,6–11]

The ICM method allows the production of very thin MSCs with about 0.1 mm in diameter and high aspect-ratio (ap. 800), which are more adequate for mechanical reinforcement uses.[4,12–15] In this technique, a molybdenum block with parallel channels is infiltrated with an oxide melt by capillarity and thousands of single crystal fibres are therefore produced simultaneously. After solidification, molybdenum is dissolved in a mixture of acids to release the fibres. These materials were able to attain lengths up to 80 mm, being considered chemically homogeneous and inclusion-free. The ICM made fibres are formed by an assemblage of consecutive single crystal areas with up to 5 mm in size and with misorientations of the *c*-axis of about 3° in relation to the fibre axis.[4] Glassy inclusions are present on the fibres periphery, decreasing their creep resistance above 1500 °C.[12]

Sayir and Farmer[16] employed the laser floating zone (LFZ) method to produce single crystalline oxide fibres with 200 mm in length and 0.15 mm in diameter from aluminosilicate melts. The directionally solidified fibres with 2:1 nominal composition, grown from 3:2 ($3Al_2O_3{\cdot}2SiO_2$) feed rods, were strongly faceted with steep changes in the fibre diameter (usually termed as "bamboo-like"). The facets act as critical flaws limiting the fibre strength at room temperature (tensile strength ~1.15 GPa). However, at 1450 °C, the mullite fibres still exhibit 80% of tensile strength at room temperature. TEM revealed that these mullite single crystals are free of dislocations, low-angle boundaries and voids, but still contain gas bubbles. Silicate glass films frequently encase the mullite crystals. The same fibre growth technique allowed the production of 500 μm diameter mullite fibres with the same 3:2 composition, for a complete assessment of mullite single crystals elastic constants.[17] A similar method to the previous one, involving also local melting, makes use of a quadrupole lamp.[3] A disc-shaped hot zone was used to produce mullite whiskers with elongated grains of about 400 μm in length, aligned along the fibre axis. A bamboo-like microstructure was obtained after repeated heat treatment cycles of a whisker-templated fibre.

In this study, the LFZ fabrication technique was used to grow 2:1 mullite single crystals and textured polycrystalline mullite fibres with millimetric diameters like in Czochralski method, but at a higher growth rate, between 10 and 100 mm/h. The influence of the process conditions on the microstructural features and mechanical properties at room temperature will be presented and discussed.

2. Experimental

Feed and seed rod precursors for LFZ growth were prepared by mixing, in an agate ball mill, alumina (Merck anhydrous γ-alumina) and silica (Aldrich 99%) powders in 77:23 wt.% Al_2O_3:SiO_2 proportion (2:1 M). Polyvinyl alcohol was added to bind the powder mixture (PVA 0.1 g/ml) that was further extruded into cylindrical rods with diameters in the range of 1.40–1.85 mm.

The LFZ apparatus comprises a 200 W CO_2 laser (Spectron). A circular crown-shaped laser beam was used to melt the top of the feed rod. The seed rod was immersed into the molten zone and pulled downwards at three distinct pulling rates: 10, 40 and 100 mm/h. Fibres with diameters in the range of 1.2–1.6 mm were obtained in air at atmospheric pressure.

X-ray diffraction experiments were carried out with a Bruker-AXS D8 Discover apparatus using the Cu Kα1 line collimated with a Göbel mirror, an asymmetric 2 bounce Ge(2 2 0) monochromator and a divergent slit of 1.5 mm. Two different measurements were performed on each sample: (i) detector scan with the fibre rotating along its grown axis, in order to check the crystalline orientation; (ii) rocking curves (RC) combined with the Bond Method, in order to determine the lattice parameter and crystalline quality.

Fibre microstructure and phase development were characterized by scanning electron microscopy (Hitachi S4100) with energy dispersive spectroscopy (SEM/EDS) on polished surfaces of longitudinal fibre section. A Raman spectrometer (Jobin Yvon HR800, Horiba) with a He:Cd laser at 325 nm of (Kimmon) was used to characterized the Raman signal of the fibres in two perpendicular directions.

An universal mechanical testing machine (Zwick, model BT1-FR020TNA50) with 20 kN of maximum load was used to evaluate the flexural strength, σ, of the LFZ grown fibres. The σ value was assessed by four point bending test at RT in samples with at least 30 mm in length, using the equation:

$$\sigma = \frac{8F(L_1 - L_2)}{\pi D^3} \quad (1)$$

where F is the applied load, L_1 (25.4 mm) and L_2 (11.0 mm) the distances between exterior and interior contact points and D the fibre diameter.

Vickers indentation experiments on polished surfaces were carried out in a Shimadzu M apparatus, under 9.8 N of load (F) during 15 s, at room temperature. This way, the indentation fracture toughness of the fibres, K_{IC}, was estimated from Anstis' equation[18]:

$$K_{IC} = 0.016\left(\frac{E}{H_V}\right)^{1/2}\left(\frac{F}{C^{3/2}}\right) \quad (2)$$

where E is the Young's modulus, H_V the Vickers hardness and C is the average length of cracks emerging from indentation corners.

The hardness and Young's modulus were measured by ultra-microindentation in a Fischerscope H100 apparatus. Each value results from an average of 10 indentations performed under the applied load of 1 N in the longitudinal fibres direction. All data were corrected for the geometrical imperfections of the Vickers indenter, the thermal drift of the equipment, and the uncertainty in zero position following the method proposed by Antunes et al.[19]

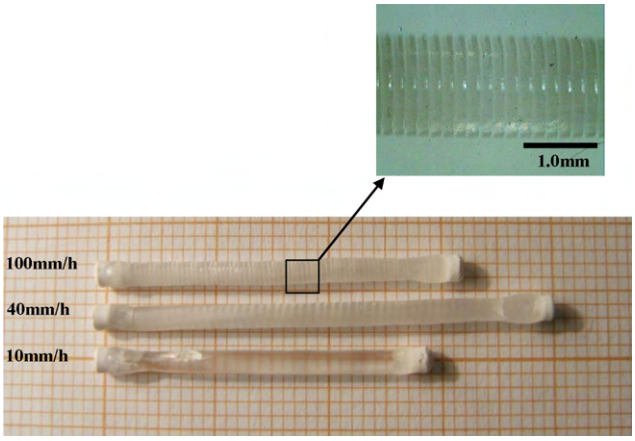

Fig. 1. Macrograph view of the mullite fibres grown at distinct pulling rates, evidencing translucency and transparency features. Notice the 1 mm background mesh.

3. Results

3.1. Microstructural and phase characterization

The visual inspection of the LFZ mullite grown fibres allowed to distinguish a first characteristic as a function of the pulling rate: at the lowest value of 10 mm/h, the fibres are transparent, while at higher pulling rates they become translucent (Fig. 1). Another macroscopic characteristic is the screw-shaped configuration of the fibres' surface, as can be seen in the inset of Fig. 1.

Powder XRD spectra after milling (Fig. 2a) confirm that the fibres are crystalline and monophasic in nature. Mullite has the 2:1-composition, as the experimental spectra fit well with that of $Al_{2.4}Si_{0.6}O_{4.8}$ stoichiometry (ICDD 73-1389). The corresponding XRD spectra of the pristine fibre (Fig. 2b) revealed the absence of most of the 2:1 mullite peaks. As the experimental data were taken from the surface of the rotating fibres and only the ($h\,k\,0$) reflections are present, it is possible to conclude that fibre axis is [0 0 1] oriented.

To elucidate if the fibre is single or the polycrystalline, XRD rocking curves were performed, leading to results like those presented in Fig. 3. For the fibre grown at the slowest pulling rate (10 mm/h), all the rocking curves, in direct and inverse geometries around [0 0 2] and [6 0 0] directions, present only one narrow peak (Fig. 3a and b). This demonstrates that such fibres are single crystals with excellent crystalline quality. On the contrary, the fastest grown fibres (100 mm/h) show high mosaicity in all directions, as denoted by the presence of several peaks in all RCs (Fig. 3c and d). The mosaics' spread is about 0.5° tilted on [0 0 1] direction and ~7° twisted on the same direction. The RC curves in the fibres grown at the intermediate pulling rate (40 mm/h) also denote a polycrystalline character. The lattice parameters calculated by the Bond Method in the single crystal fibres are: $a = 7.681$ Å; $b = 7.587$ Å; $c = 2.887$ Å. The deviation of these values to those of the ICDD file is within the experimental error (0.003 Å).

SEM observations (Fig. 4) on the polished longitudinal sections of the mullite fibres confirm the above reported charac-

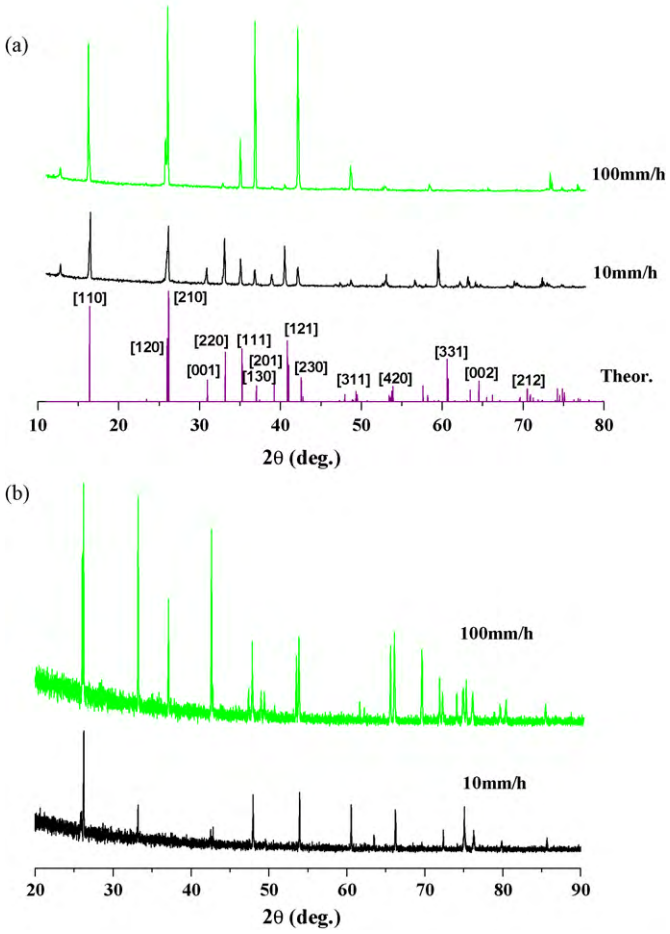

Fig. 2. XRD spectra of fibres grown at 10 mm/h and 100 mm/h taken from the: (a) powder form after fibre crushing and (b) integral fibre.

teristics, namely the strong influence of the pulling rate on the crystalline nature. In the micrographs of the fibre grown at the slowest speed (10 mm/h, Fig. 4a) small imperfections with linear appearance in cross-section are visible inside the uncontrasted matrix, orientated in parallel to the fibre axis. In contrast, very well-defined parallel crystals are visible in the 100 mm/h grown fibres (Fig. 4c). These crystals are very long, regularly developed to almost all the fibre length with a width of about 12 μm. In the intermediate case, the fibre grown at 40 mm/h (Fig. 4b), the microstructure is characterized by a less regular growth of several crystals. Besides its poorer alignment, the crystals are wider than those in the fastest fibre. EDS analysis (Fig. 5) performed at the grain boundaries and the lamellar inclusions of the single crystals reveals that these are Si-enriched compared to the crystal matrix composition.

The SEM analysis of the fractured surfaces, Fig. 6 reveals the absence of pores in the interior of the fibres, both in transverse and longitudinal directions. Mullite, as a ceramic material, fails by brittle fracture mode, as can be illustrated by the characteristic "river marking" pattern in Fig. 6c and d. This topographic feature results from crack stepping between parallel planes inside every crystal. The analysis of the transverse section, presented in Fig. 6c, confirms the crack propagation in different direc-

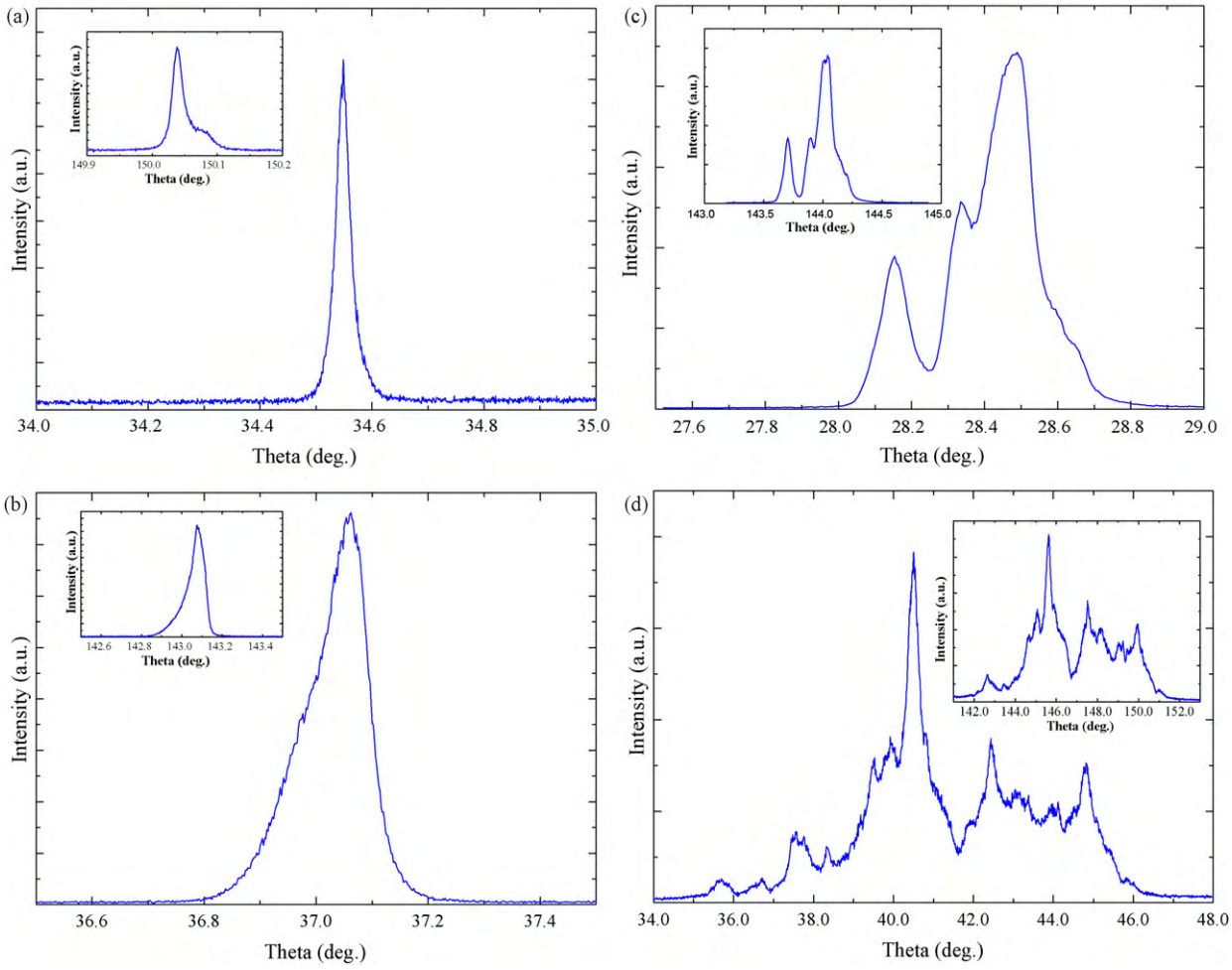

Fig. 3. XRD rocking curves of: (a) (0 0 2) plane of fibre grown at 10 mm/h; (b) (6 0 0) plane of fibre grown at 10 mm/h; (c) (0 0 2) plane of fibre grown at 100 mm/h; (d) (6 0 0) plane of fibre grown at 100 mm/h. The insets correspond to the inverse geometry.

tions according to the orientation of the ($h\,k\,0$) planes in each grain.

Raman spectra were acquired from the lateral surfaces, having the fibres positioned in two perpendicular directions, one of them parallel to the laser polarization. The spectra taken from the 40 mm/h fibre are presented in Fig. 7. Seven characteristic vibration modes are patent, corresponding to the mullite signature[20–22]: 313, 412, 615, 727, 873, 960 and 1138 cm^{-1}. The changes observed in the spectra obtained in perpendicular directions are another evidence of fibre texturing, corroborating the XRD and SEM analysis.

3.2. Mechanical behaviour

The flexural strength (σ) of mullite fibres pulled at different rates is plotted in Fig. 8. According to the results, the best behaviour corresponds to the most regular polycrystalline fibres (Fig. 4c), those grown at the highest pulling rate (100 mm/h). Fibres pulled at 40 mm/h are also polycrystalline in nature but less regular in both crystal dimensions and alignment (Fig. 4b), showing a higher dispersion of values. Single crystalline fibres are the less resistant ones. The average indentation fracture toughness (K_{IC}) values vary within the range 6.2–8.8 MPa $m^{1/2}$ (Fig. 8). Again, there is a net difference between the single and the polycrystalline fibres, the former presenting higher brittleness.

Ultramicrohardness and Young's modulus results are given in Fig. 9. Both properties show a slight trend to decrease with the pulling rate, contrarily to the mechanical properties mentioned before. The best results of H_V and E were found for the fibres pulled at the slowest pulling rate, 10 mm/h.

4. Discussion

4.1. Microstructure and phase development

The LFZ technique has been widely used to grow single crystals or textured polycrystalline fibres during the last two decades. However, its application to mullite fibres is scarce, probably due to the difficulty to obtain regular fibres without internal defects.[16] Several growth conditions were tried in order to ascertain the appropriate procedure that permitted to produce macroscopically uniform and straight fibres, namely downward and upward pulling, growth with or without seed and feed rod

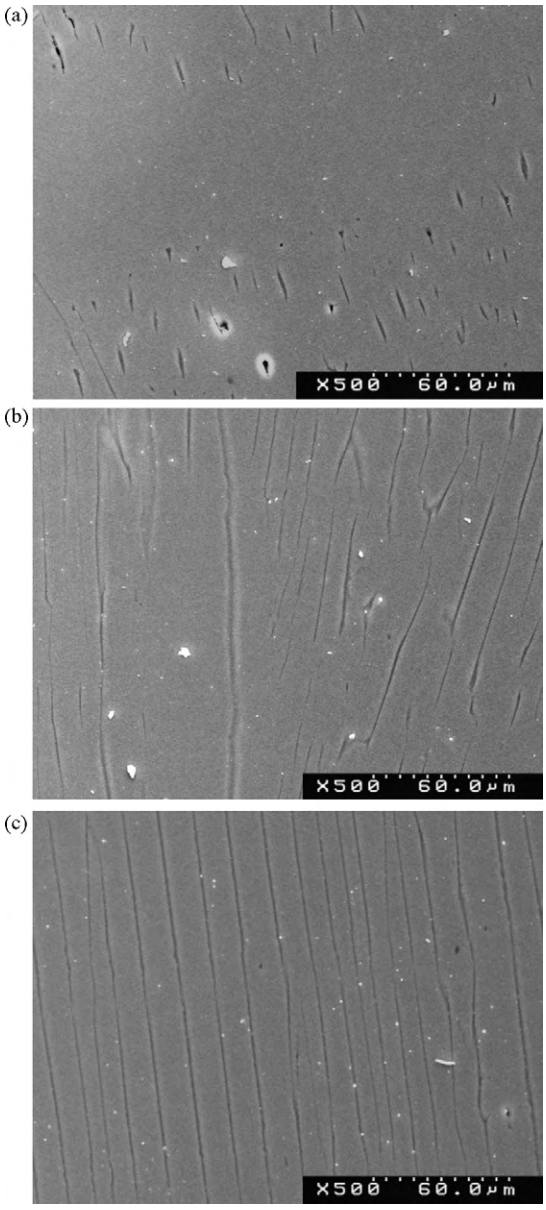

Fig. 4. SEM micrographs of longitudinal sections of mullite fibres grown by LFZ at (a) 10 mm/h, (b) 40 mm/h, and (c) 100 mm/h.

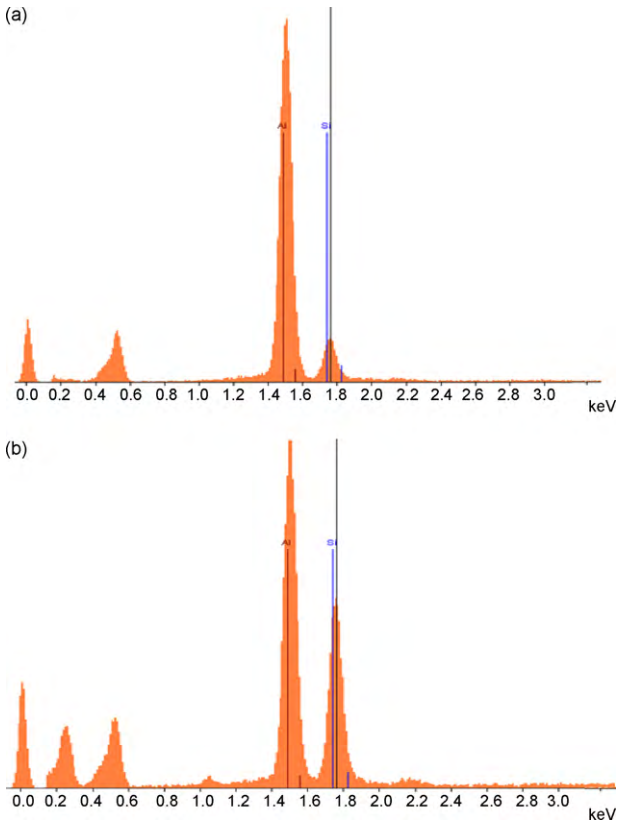

Fig. 5. EDS spectra of the matrix (a) and the intergranular phase (b) of a fibre grown at 100 mm/h.

rotation, rotation in opposite or in the same direction, etc. Particularly, upward growth leads to high porosity due to ascending gas bubbles from the organic binder that are trapped in the solid fibre. The best fibres were grown downwards, having the feed and the seed rods slowly rotating in opposite senses.

The transparency degree of fibres pulled at different rates (Fig. 1) becomes from their single crystalline or polycrystalline character as demonstrated by the XRD analysis. Indeed, the XRD spectra (Figs. 2 and 3) of the slowest pulled fibre (10 mm/h) denoted that this was a growth condition for development of single transparent crystals, while higher pulling rates lead to polycrystalline translucent fibres. The inset in Fig. 1 shows the occurrence of surface striations perpendicularly to the fibre axis. Growth striations have been observed in high melting-point materials such as Al_2O_3[23] and their origin has been attributed to thermal asymmetry in the melt due to displacement of the rotation axis from the thermal centre.

The single or polycrystalline character of the mullite fibres can be observed in the respective SEM micrographs (Fig. 4). For high pulling rates (100 mm/h), the obtained morphology is a good example of cellular growth (Fig. 4c). This feature is explained by the Burton, Primm and Slichter (BPS) theory which states the breakdown of the planar solid/liquid interface when high pulling rates are used, due to constitutional supercooling.[24] When this condition is established, the increase of the pulling rate results in a decrease of the intercellular spacing (λ) according to the equation:

$$\lambda_i \approx 2\pi \left(\frac{D\Gamma}{k\Delta T_0 v_f} \right) \quad (3)$$

Where D is solute diffusion coefficient, Γ the Gibbs–Thomson coefficient, ΔT_0 the undercooling, v_f the pulling rate and k the effective distribution coefficient.

This equation also explains why wider crystal diameters are obtained in the fibres pulled at 40 mm/h (Fig. 4b) than in those pulled at 100 mm/h (Fig. 4c). When lower pulling rates are used, as is the case of the 10 mm/h pulled fibre, planar growth takes place according to the BPS theory, leading to single crystal development (Fig. 4a). Moreover, the absence of grain boundaries results in good transparency degree as it is shown in Fig. 1. However, at a microscopic level, these fibres present Si-rich internal defects in accordance to previous research works,[25]

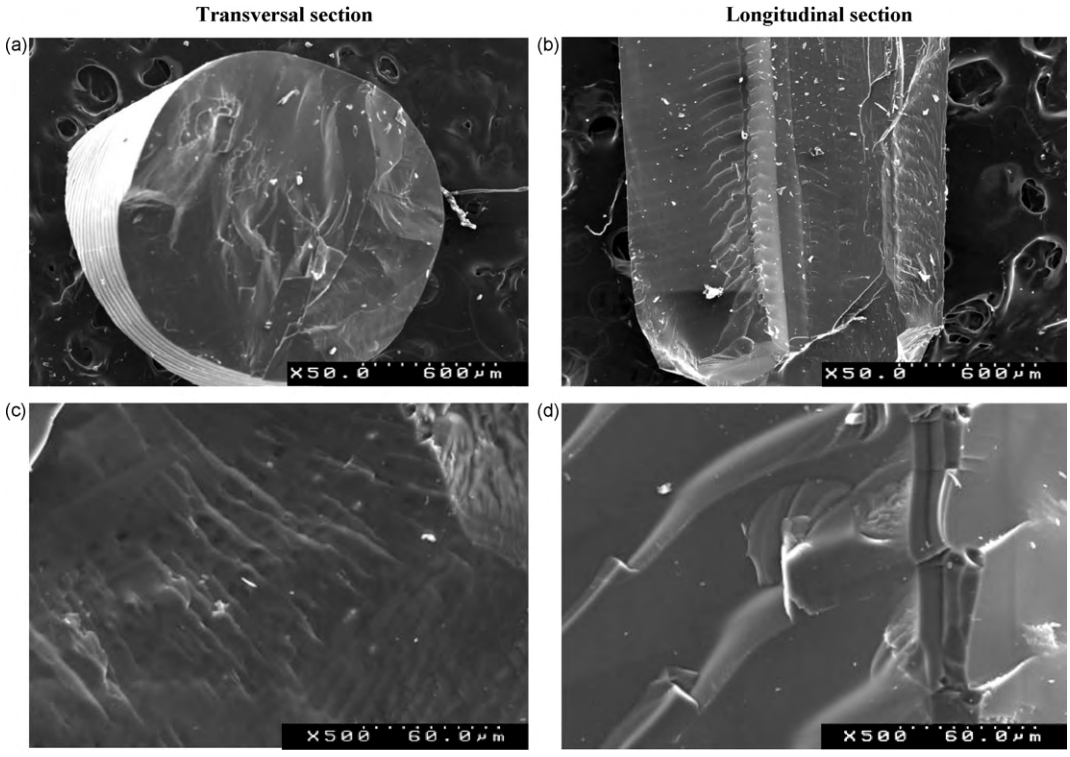

Fig. 6. SEM micrographs of the transversal (a, c) and longitudinal (b, d) cross-sections of the fibre grown at 40 mm/h.

being considered as lamellar inclusions. In the polycrystalline fibres, these Si-rich grain boundaries have been reported as an aluminosilicate glass,[16] more prone to produce light scattering, increasing opacity and rendering such fibres only translucent.

Both the polycrystalline and the single crystal fibres uniquely presented 2:1 mullite crystals, following the nominal composition of the seed and feed rods. Mullite exhibits an oxygen deficient orthorhombic structure covering a wide solid solution with $Al_{4+2x}Si_{2-2x}O_{10-x}$ composition (oxygen vacancies x between 0.2 and 0.9).[2] Different types of mullite can be obtained according to distinct synthesis procedures. When mullite materials are obtained via crystallization of aluminosilicate melts, the supersaturated Al_2O_3-rich 2:1-composition is preferred.[2]

The favourable [0 0 1] orientation along the fibre axis (Fig. 3) is the result of the surface energy competition between the $\{h\,k\,0\}$ and the (0 0 1) planes and of the respective growth rates. Mullite exhibits strong bond chains parallel to the c-axis resulting in higher surface energy in (0 0 1) than in $\{h\,k\,0\}$ planes2. Moreover, in the present system the highest growth direction is [0 0 1], the slowest growing planes dictating the crystals habit. As a consequence, $\{h\,k\,0\}$ become the long-prismatic planes of the mullite crystals. This feature is similar to the development of acicular mullite crystals having their needle axis parallel to the

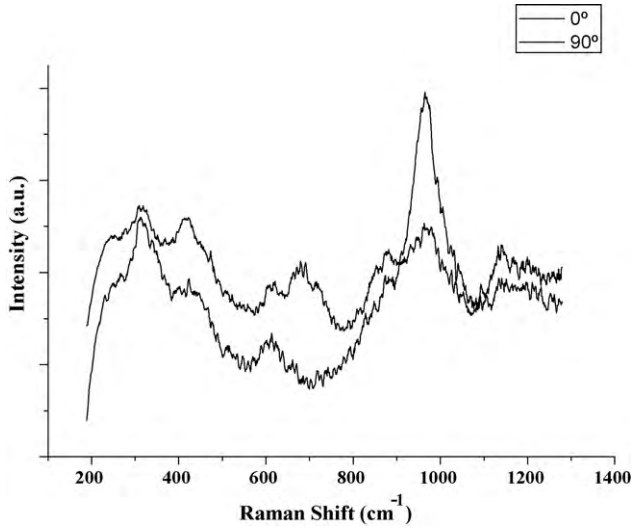

Fig. 7. Raman spectra acquired at two perpendicular directions in a fibre grown at 40 mm/h.

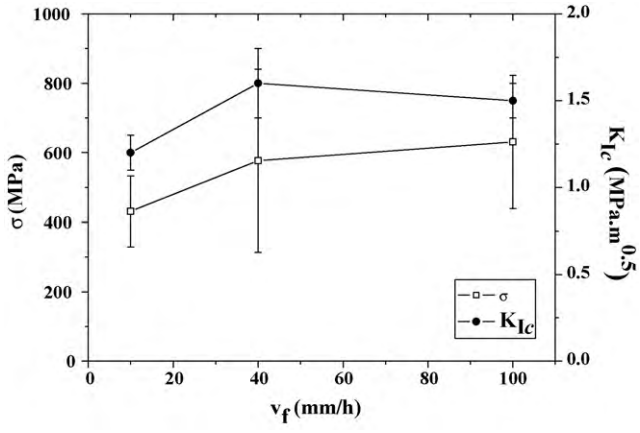

Fig. 8. Flexural strength values (σ) and fracture toughness values (K_{IC}) for fibres grown at 10 mm/h, 40 mm/h, and 100 mm/h.

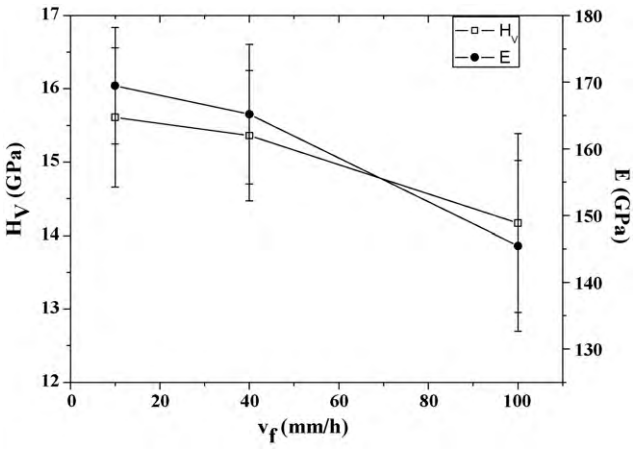

Fig. 9. Evolution of hardness and Young's modulus relative to the mullite fibres grown at 10 mm/h, 40 mm/h, and 100 mm/h.

crystallographic *c*-axis, that were also grown from aluminosilicate melts.[2]

The growth anisotropy was confirmed by comparison of the Raman spectra of the same fibre obtained in two perpendicular directions (Fig. 7). A previous Raman study of 2/1 mullite single crystals under different polarized conditions demonstrated that the intensities of the bands are a function of the angle between the electrical field vector $\vec{E}$ associated to the incident laser beam and the crystallographic direction.[21] Spectra obtained in that study for $\vec{E}$ ||[1 0 0] and $\vec{E}$ ||[0 0 1] are similar to 0° and 90° ones in Fig. 7, respectively, corroborating the present [0 0 1] fibre axis alignment.

4.2. Mechanical properties

A direct comparison of the flexural strength data plotted in Fig. 8 to the literature values is not possible because only tensile and compressive test results have been reported. Moreover, the fibre dimensions in those works differ from the present ones. Sayir et al.[16] tested LFZ grown 3:2 mullite fibres with one order of magnitude smaller diameters (ap. 150 μm) whose tensile strength varied between 553 and 630 MPa. The assignment of the mechanical data to single or polycrystalline fibres is not straightforward although the single crystals seem to be the most resistant in such research work (630 MPa). The average flexural strength of the mullite single crystals in the present work is 431 MPa, as given in Fig. 8. This lower value, in comparison to those reported in the literature, could be a consequence of the higher volume of the present fibres and thus of the higher internal number of defects (Weibull statistics). Moreover, it is well known that, as the fibre diameter approaches the achievable maximum of the growth technique, the residual stresses increase.[26]

Contrary to the work by Sayir et al., our polycrystalline fibres are stronger than the single crystals ones (Fig. 8). The flexural strength values are within the same error range in both 40 and 100 mm/h grown fibres, amounting to ~600 MPa, Fig. 8. The superior behaviour of the polycrystalline fibres could be attributed to their well-defined regular structure (Fig. 4b), whereas the single crystals present lamellar inclusions (Fig. 4a) that act as crack nucleation agents and thus decrease the fibre strength. The obtained average flexural strength value is similar to the corresponding tensile strength of 553 MPa obtained by Sayir et al., but less than the $\sigma = 812$–994 MPa reported in the same work for polycrystalline 2:1 mullite fibres grown by the Edge-Defined Film Fed Growth technique. Again, it must be pointed out that the diameter of these fibres is one order of magnitude smaller (ap. 150 μm) than that of the present ones.

As it can be seen in the graph of Fig. 8, the data dispersion in the present set of samples is relatively high. The maximal flexural strength values for single and polycrystalline fibres are 579 and 1060 MPa, respectively. This means that it will possible to significantly improve the mechanical behaviour if the intrinsic fibre quality is enhanced. A route for that could be a second growth run using the as-grown fibres as feed rods,[16] which will be subject of a further study.

The indentation fracture toughness (K_{IC}) results in Fig. 8 corroborate the higher brittleness of the single crystalline fibres (average value of $K_{IC} = 1.2\ \text{MPa m}^{1/2}$), which are almost 30% weaker than that of the polycrystalline ones ($K_{IC} = 1.6\ \text{MPa m}^{1/2}$). In the case of the polycrystalline fibres, the grain boundaries further contribute to the K_{IC} by providing a crack-arresting effect, contrary to the free crack growth in single crystals. There are no reported values in the literature for the K_{IC} of mullite fibres, although a value of 2.8 MPa.m$^{1/2}$ was reported for polycrystalline materials obtained by conventional powder technology.[1]

The ultramicrohardness does not vary significantly for all fibres, albeit it decreases from an average value of 15.6 GPa for the single crystalline one to 14.2 GPa for that grown at 100 mm/h (Fig. 9). The indentation imprints have diagonal lengths of about ~10 μm, most probably intersecting a grain boundary in the former polycrystalline ones (Fig. 4). This denotes the relevance of the glassy grain boundary that possesses an intrinsic lower hardness. A similar contribution of such amorphous phase explains the lowest Youngĭs modulus of the 100 mm/h grown fibre (Fig. 9). The microhardness of single crystal mullite was determined by several authors[11,17,27] yielding a value of about 15 GPa, while the microhardness of polycrystalline mullite ceramics is reported to be lower (10–14.5 GPa) due to presence of glassy phases at grain boundaries.[28]

5. Conclusions

Laser floating zone technique allowed growing of relatively large 2:1 mullite fibres ($L = \sim 40$ mm, $\varnothing = \sim 1.6$ mm) with single or polycrystalline nature. The former were obtained at 10 mm/h, while the later resulted from higher puling rates, 40 and 100 mm/h. It is worth to note that it was possible to grow single crystals using an extruded bar as seed material, and not necessarily a single crystal seed. In spite of that, all growth conditions resulted in mullite crystals [0 0 1] oriented along the fibre axis.

The single crystalline fibres are less mechanically resistant than the polycrystalline ones: average flexural strength values

of 431 MPa and fracture toughness of 1.2 MPa.m$^{1/2}$, for single crystals; 631 MPa and 1.6 MPa.m$^{1/2}$, for polycrystalline fibres. On the contrary, both the hardness and Young's modulus values determined by ultramicroindentation technique are superior in the single crystals: $H_V = 15.6$ GPa and $E = 170$ GPa, against $H_V = 14.2$ GPa and $E = 145$ GPa in the polycrystalline fibres. The lower mechanical resistance of the single crystalline fibres is attributed to the presence of lamellar inclusions, while the intergranular glassy phase in the polycrystalline fibres explains their lower hardness and elasticity modulus.

Acknowledgments

The authors acknowledge FCT for the financial funding from PTDC/CTM/66195/2006 project.

References

1. Schneider H, Komarneni S, editors. *Mullite*. Weinheim: Wiley VCH; 2005.
2. Schneider H, Schreuer J, Hildmann B. Structure and properties of mullite - a review. *J Eur Ceram Soc* 2008;**28**:329–44.
3. Yoon W, Sarin P, Kriven WM. Growth of textured mullite fibres using a quadrupole lamp furnace. *J Eur Ceram Soc* 2008;**28**:455–63.
4. Ruscher CH, Mileiko ST, Schneider H. Mullite single crystal fibres produced by the internal crystallization method (ICM). *J Eur Ceram Soc* 2003;**23**:3113–7.
5. Guse W, Mateika D. Growth of mullite single-crystals ($2A1_2O_3{\cdot}SiO_2$) by Czochralski method. *J Cryst Growth* 1974;**22**:237–40.
6. Hildmann B, Ledbetter H, Kim S, Schneider H. Structural control of elastic constants of mullite in comparison to sillimanite. *J Am Ceram Soc* 2001;**84**:2409–14.
7. Hildmann B, Braue W, Schneider H. Topotactic growth of alpha-alumina platelets on 2/1 mullite single crystal surfaces upon thermal decomposition of mullite in dry and wet atmospheres. *J Eur Ceram Soc* 2008;**28**: 407–23.
8. Schmucker M, Mechnich P, Zaefferer S, Schneider H. Water vapor corrosion of mullite: single crystals versus polycrystalline ceramics. *J Eur Ceram Soc* 2008;**28**:425–9.
9. Schreuer J, Hildmann B, Schneider H. Elastic properties of mullite single crystals up to 1400 °C. *J Am Ceram Soc* 2006;**89**:1624–31.
10. Fielitz P, Borchardt G, Schmucker M, Schneider H. Al-26 diffusion measurement in 2/1-mullite by means of Secondary Ion Mass Spectrometry. *Solid State Ionics* 2006;**177**:493–6.
11. Kriven WM, Siah LF, Schmucker M, Schneider H. High temperature microhardness of single crystal mullite. *J Am Ceram Soc* 2004;**87**:970–2.
12. Mileiko ST, Serebryakov AV, Kiiko VM, Kolchin VN, Kurlov AA, Novokhatskaya NI. Single crystalline mullite fibres obtained by the internal crystallisation method: microstructure and creep resistance. *J Eur Ceram Soc* 2009;**29**:337–45.
13. Kiiko VM, Mileiko ST. Evaluation of the room-temperature strength of oxide fibres produced by the internal-crystallization method. *Compos Sci Technol* 1999;**59**:1977–81.
14. Mileiko ST, Kiiko VM, Yu VM, Starostin AA, Kolchin VN, Kozhevnikov LS. Fabrication and some properties of single crystalline mullite fibres. *Scripta Mater* 2001;**44**:249–55.
15. Ruschera CH, Mileiko ST, Schneider H. Mullite single crystal fibres produced by the internal crystallization method (ICM). *J Eur Ceram Soc* 2003;**23**:3113–7.
16. Sayir A, Farmer SC. Directionally solidified mullite fibres. In ceramic matrix composites—advanced high temperature structural materials. *Mat Res Soc Symp Proc* 1995;**365**:11–20.
17. Kriven WM, Palko JW, Sinogeikin S, Bass JD, Sayir A, Brunauer G, et al. High temperature single crystal properties of mullite. *J Eur Ceram Soc* 1999;**19**:2529–41.
18. Anstis GR, Chantikul P, Lawn BR, Marshall DB. A critical evaluation of indentation techniques for measuring fracture toughness: I. Direct crack measurements. *J Am Ceram Soc* 1981;**64**:533–8.
19. Antunes JM, Cavaleiro A, Menezes LF, Simões MI, Fernandes JV. Ultramicrohardness testing procedure with Vickers indenter. *Surf Coat Technol* 2002;**149**:27–35.
20. Volla D, Angererb P, Berana A, Schneider H. A new assignment of IR vibrational modes in mullite. *Vibrat Spectrosc* 2002;**30**:237–43.
21. Ruscher C. Phonon spectra of 2:1 mullite in infrared and Raman experiments. *Phys Chem Miner* 1996;**23**:50–5.
22. Liem N, Sagon G, Quang V, Tan H, Colomban P. Raman study of the microstructure, composition and processing of ancient Vietnamese (proto)porcelains and celadons (13–16th centuries). *J Raman Spectrosc* 2000;**31**:933–42.
23. Cockayne B, Gatesockayne MP. Growth striations in vertically pulled oxide and fluoride single crystals. *J Mater Sci* 1967;**2**:118–23.
24. Flemings MC. *Solidification processing*. New York: McGraw-Hill; 1974.
25. Dokko PC, Pask JA. High-temperature mechanical properties of mullite under compression. *J Am Ceram Soc* 1977;**60**:150–5.
26. Brice JC. The cracking of Czochralski-grown crystals. *J Cryst Growth* 1977;**42**:427–30.
27. Kollenberg W, Schneider H. Microhardness of mullite at temperatures to 1000 °C. *J Am Ceram Soc* 1989;**72**:1739–40.
28. Somiya S, Davis RF, Pask JA, editors. *Mullite and mullite matrix composites*. Berkeley: Ceramics Transactions; 1990.